CHARACTERIZING FLUID PRESENCE AND TRANSPORT IN ROCK CORES AT RESERVOIR-LIKE CONDITIONS VIA SPATIALLY RESOLVED NMR RELAXATION/DIFFUSION MAPS

Huabing Liu[1], Mark Hunter[1,2], Sergei Obruchkov[1], Evan McCarney[2], Mitch Robison[3], Robin Dykstra[1,2], Petrik Galvosas[1]
[1] Victoria University of Wellington, SCPS, MacDiarmid Institute for Advanced Materials and Nanotechnology, Wellington, New Zealand,
[2] Magritek Ltd., Wellington, New Zealand
[3] University of Auckland, Auckland, New Zealand

This paper was prepared for presentation at the International Symposium of the Society of Core Analysts held in St. John's Newfoundland and Labrador, Canada, 16-21 August, 2015

ABSTRACT
The properties of fluids saturating rocks depend strongly on temperature and pressure. Therefore, ambient laboratory conditions may not be desirable for the investigation of fluids in reservoir rocks. To mimic the reservoir, a pressurized and temperature controlled (overburden) cell, compatible with Nuclear Magnetic Resonance (NMR), was assembled within a 2 MHz NMR Rock Core Analyzer. 1D NMR relaxation and 2D diffusion-relaxation correlation distributions of fluid-saturated rock cores were measured in conjunction with 1D NMR imaging. By performing these spatially resolved NMR relaxometry and diffusometry experiments within the environment of the overburden cell, it is possible to obtain porosity, fluid saturation and residual fluid content profiles under reservoir-like conditions. Here we show for the first time that these spatially resolved NMR relaxometry and diffusometry experiments could be performed under elevated pressures and temperatures for fluids flooding rock cores in the laboratory. Experiments performed with this NMR setup may allow one to study the oil properties under reservoir conditions, which may inform oil recovery enhancement strategies.

INTRODUCTION
NMR is one of the non-invasive techniques to deliver substantial petrophysical parameters, such as pore volume, permeability and fluid saturation in rock plugs [1]. In particular, low-field ^{1}H NMR has become an important tool to study rock core plugs from oil reservoirs, and is established as an industry standard to calibrate NMR well-logging data [2]. In this context, the relaxation time/diffusion coefficient distributions, as well as their multi-dimensional correlation maps, are routinely utilized to characterize pore size, wetting state, fluids types, and quantify individual fluid phase saturations [3-5]. Meanwhile, magnetic resonance imaging (MRI) was introduced in rock core analysis to monitor "real-time" fluid invasion profiles during core flooding experiments [6]. To reveal the spatial fluid properties with saturating/flooding multi-phase fluids, it is desirable to combine NMR imaging techniques with 1D relaxation time/diffusion coefficients or 2D diffusion-relaxation correlation measurements. Subsequently, it allows one to extract the local profiles of

pore structure, saturation of individual fluid phases as well as wettability information [7-9].

Most reservoir rocks are buried in the formation approximately thousands meter deep, where the *in-situ* temperatures and pressures are much higher as compared to conditions on the surface [10, 11]. In this case, fluid properties (*e.g*. viscosity) in porous rocks behave differently according to local pressure and temperature, leading to a complex mechanism of oil recovery in oilfields [12]. Therefore, in order to characterize and model fluid properties and transport, it is necessary to confine and flush rock cores at reservoir-like temperatures and pressures whilst NMR experiments are performed in laboratory measurements.

In this work, an overburden system was assembled to pressurize rock cores at required temperatures and pressures. Furthermore, spatially resolved NMR techniques were combined with relaxation time (T_1 and T_2) and relaxation-diffusion correlation (D-T_2) experiments and implemented on a low-field NMR rock core analyzer. Since NMR signal intensity is inversely proportional to temperature, imaging was restricted to one dimension (1D) only, to ensure sufficient Signal-to-Noise Ratio (SNR). The property and distribution of oil saturating rock core were studied at different temperatures before flooding experiment. Subsequently, the conditions of secondary oil recovery were investigated by flooding water through an oil-bearing rock plug.

HARDWARE CONFIGURATION

A commercial 2 MHz NMR analyzer equipped with a shielded 1D gradient coil (Magritek, Ltd.) is used to acquire NMR data in this work [13]. The RF probe has a dimension of 10 cm length and 5.4 cm diameter. This setup is complemented with a Daedalus Innovations overburden rock holder (Figure 1 a), which maintains required temperatures and pressures for the rock plug under study [14]. It is worth noting that the materials of the rock holder, especially the section close to the detection volume of the NMR system, are chosen to be non-magnetic to avoid disturbing NMR signals.

Before the experiments, the rock core is placed between two PEAK mounts first, wrapped by heat shrink sleeve, and then loaded in the chamber of overburden holder (Figure 1 a). Two parts are screwed in each end of the holder housing to seal the overburden cell. Subsequently, the overburden cell within rock plug is inserted in the bore of NMR system, and is connected to two external circuits. These two circuits will provide pressurized fluid flooding through rock samples (left plumbing in Figure 1 b), and the confining pressure and temperature for rock plug (right loop in Figure 1 b), respectively. To achieve the desired confining temperature and pressure for the rock plug, two ISCO syringe pumps are used to drive confining fluid flow (right part in Figure 1 b). Perfluro polyether (PFPE, non-hydrogen signal) is chosen as the confining fluid to circulate in the plumbing and rock holder chamber. A heating bath after the syringe pump ensures the required temperature of PFPE before entering the pressure cell. Another bath after the cell will cool down the confining fluids before entering a back pressure regulator (BPR 1) which controls the pressure surrounding the rock core. On-site pressures and temperatures are logged to monitor the real-time confining conditions of the loaded rock core. Furthermore, a high-pressure crank

pump is connected to the inlet end of the flooding channel of the overburden rock holder to provide flooding conditions. Water can be imbibed and then pressurized through the rock core in this work.

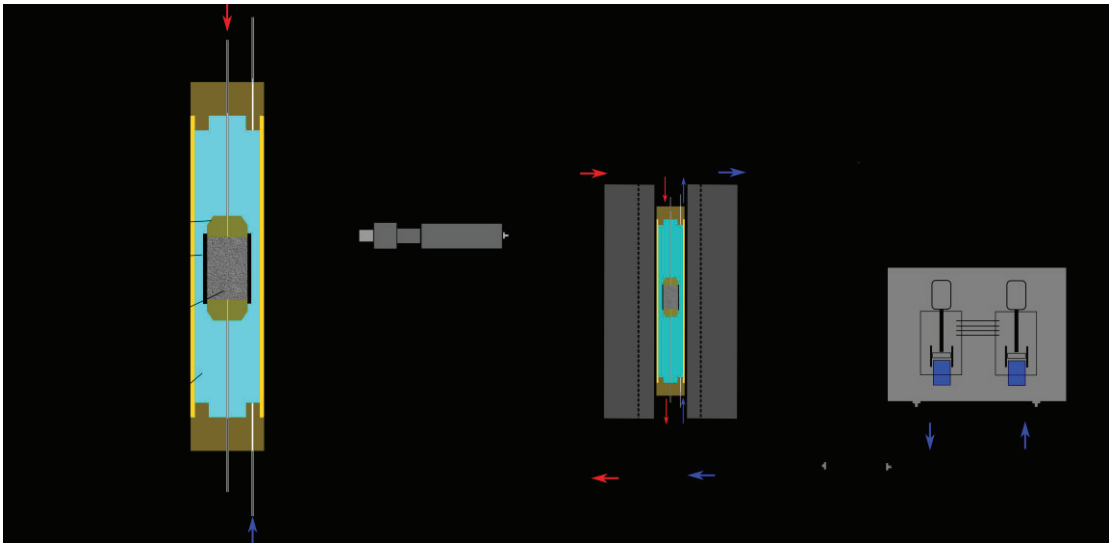

(a) (b)

Figure 1. Schematic of overburden rock holder (**a**) and its combination with low-field NMR system for high pressure and temperature experiments (**b**). Red and blue arrows indicate the flow direction of flooding fluid and confining fluid, respectively. The bold line in the confining part represents the tubing insulation. P in the circuit stands for pressure gauge and T for thermocouple.

Thermal conditions arising from the core holder within the NMR system have been modeled and simulated for different temperatures with SolidWorks. Results obtained by these simulations confirm the compatibility between operational NMR system and the overburden system.

NMR METHODOLOGIES

MRI methods are generally based on either frequency or phase encoded imaging [15]. A magnetic field gradient is applied during signal acquisition for frequency encoded imaging, ensuring spatially distributed resonance frequencies which return the image of the sample upon Fourier transform of the acquired MRI signal. The field of view (FOV) for this imaging method is determined to be: $2\pi/\gamma g\Delta t$, where g is the gradient strength and Δt is the time interval between neighboring acquired points (aka dwell time). In order to obtain an image using the phase encoded MRI method, a set of gradients within variable amplitudes is applied during a fixed time period δ before acquisition. This returns a set of experiments with varying phases in the acquired MRI signal, which again provides an image after Fourier transform. In this case, the FOV is determined as $m\pi/\gamma g_{max}\delta$ with g_{max} being the maximum intensity of the phase gradient. The imaging resolution ΔZ is FOV/m, where m is the number of acquired points in frequency-encoded imaging and the number of gradient steps in phase encoded imaging, respectively.

Since the spatial information can be encoded in a one-shot signal acquisition under fixed amplitude of the imaging gradient, frequency-encoded methods are generally faster as compared to phase-encoded. However, T_2 effects will irreversibly impact the

obtained imaging profile during the acquisition time, leading to the absence of signal with short T_2 relaxation time. The phase-encoded method on the other hand uses short signal acquisition time on the cost of experimental time, and can therefore offer more accurate imaging profiles. Both methods were employed in this work, depending on required time efficiency and accuracy.

In the context of petrophysical analysis using low-field NMR measurements, the longitudinal relaxation T_1 and transverse relaxation T_2 are mostly studied for fluid-saturated rock cores. This may provide information on the pore volume and pore size distributions. The 1D phase encoded imaging technique combined with T_2 relaxation measurements, as shown in Figure 2, can yield spatially resolved T_2 profiles [16]. The first period covered by T_{E1} is the phase encoded imaging part of the experiment, providing the 1D image (profile). The following section, consisting of the 180° pulse train acquires the NMR echo decay, which is determined by the transverse relaxation T_2. Similarly, spatially resolved T_1 profiles can be obtained by measuring T_1 using inversion/saturation recovery or rapid acquisition schemes as suggested in [17, 18], again in conjunction with the 1D imaging method.

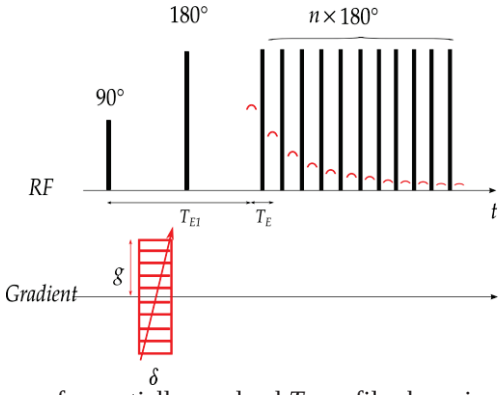

Figure 2. NMR pulse sequence for spatially resolved T_2 profiles by using phase encoded methods [16]. g is the imaging gradient which has variable intensities with a duration of δ. T_E is the echo spacing during the acquisition of the T_2 measurement.

The acquired data for spatially resolved T_2 experiments can be expressed as

$$M(k, nT_E) = \int F(z, T_2) \times e^{i2\pi kz} \times e^{-\frac{nT_E}{T_2}} dz dT_2, \quad (1)$$

while the data obtained by spatially resolved T_1 techniques (using rapid acquisition) is

$$M(k, nT_{ACQ}) = \int F(z, T_1) \times e^{i2\pi kz} \times e^{-\frac{nT_{ACQ}}{T_1}} \sin\alpha \times \cos^{n-1}\alpha \, dz dT_1 \quad (2)$$

with $k=\gamma g\delta/2\pi$. z is the gradient direction which coincides with the cylindrical axis of the rock cores in this work. α represents the small tip angle and T_{ACQ} is the signal evolution time in rapid encoding T_1 method.

Both spatially resolved T_1 and T_2 imaging methods yield two-dimensional datasets and a two-step data process is needed to extract the spatial relaxation distribution

function $F(z, T_1)$ or $F(z, T_2)$. Firstly, Fourier transform is employed to transform the encoded phase information into positions, returning the fluid content in each resolved slice (pixel). The Inversion Laplace transform algorithm is then consecutively applied slice by slice, yielding the spatial resolved relaxation distribution function. It is worth noting that $F(z, T_1)$ and $F(z, T_2)$ are akin to the curves from NMR well logging operated in the oilfield, where the sensor is pulled from the down-hole up to the surface and provide relaxation distributions from each vertical layer in the formation.
Besides relaxation measurements, diffusion coefficients of fluids can be uniquely measured by NMR techniques [15, 19]. This allows one to identify different fluid types and quantify fluid saturation in rock samples. In this case, 2D D-T_2 NMR correlation technique provides substantial information in rock core analysis, such as fluid typing and wettability identification in multi-phase experiments. Furthermore, spatially resolved D-T_2 distribution provides the aforementioned information along a certain core axis and potentially indicates progress of oil recovery or monitors the saturation level of rock cores [8]. While incorporating 2D relaxation-diffusion correlation experiment with 1D imaging technique, the entire experimental time should be taken into account for practical reasons. Therefore, the frequency encoding method is preferred because of the equivalent experimental time as compared to 2D correlation experiment without spatial resolution.

The pulse sequence for spatially resolved D-T_2 distribution is shown in **Figure 3** and the signal decay is expressed as

$$M\left(k,G,nT_E\right)=\iiint F\left(z,D,T_2\right)\cdot e^{i2\ kz}\cdot e^{\ ^{2\ 2}G^2D\left(\ \ \overline{3}\right)}\cdot e^{\ \frac{nT_E}{T_2}}\,dz\,dD\,dT_2 \qquad (3)$$

where $k=\gamma g t_p/2\pi$. Δ is diffusion observation time and δ is gradient duration. The result is a 3D data matrix acquired during the spatially resolved D-T_2 experiment. To obtain the final map, Fourier transform is performed on each acquired echo to obtain the spatial imaging profile. Then 2D ILT algorithm is applied subsequently for the 2D exponential decay data in each slice, in order to extract the local D-T_2 distribution function $F(z,D,T_2)$ [20].

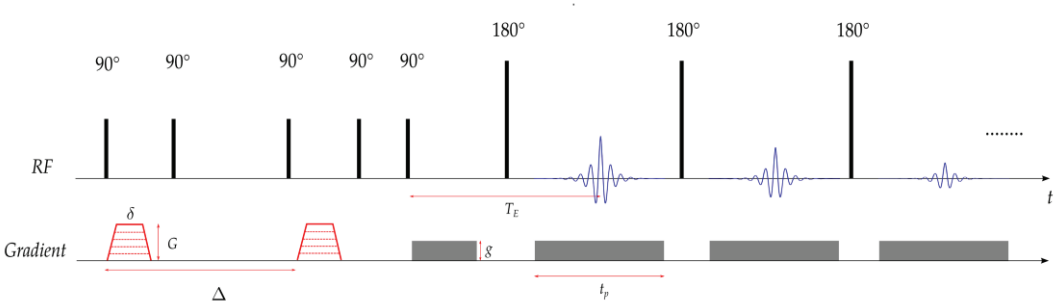

Figure 3. NMR pulse sequence for spatially resolved D-T_2 map, details are shown in [8]. Δ is the diffusion observation time and δ is the gradient duration. G and g are the gradients for encoding diffusion coefficient and position, respectively. T_E is the echo spacing and t_p is the echo acquisition time.

MATERIALS AND EXPERIMENTAL STRATEGIES

Sample. A Edwards Brown limestone core was used in this work to study fluid presence and multi-phase fluid flooding at different temperatures. The core porosity is

36.5% and the permeability is 90 mD. The rock core has a dimension of 6.3 cm length and 3.84 cm diameter. Before the experiment, the core plug was dried in an oven at 60°C for 48 h, until no hydrogen signal was detected in NMR measurements. Afterwards it was saturated with diesel (Hydrogen index HI=1.023).

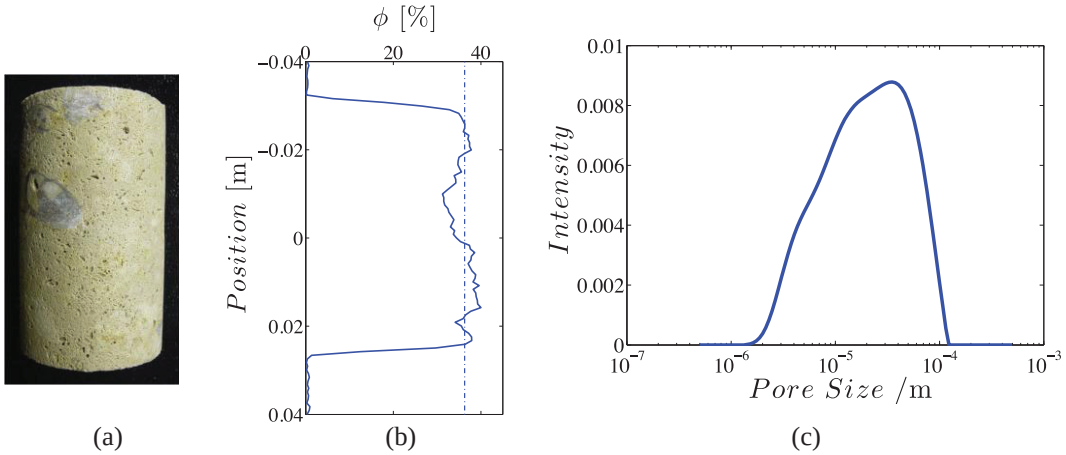

(a) (b) (c)

Figure 4. Edwards Brown plug used in this work (**a**), its porosity profile (**b**) determined by 1D imaging, and its pore length scales (**c**) determined by DDIF technique [21]. The heterogeneity of the rock sample can be recognized from the comparison of the acquired porosity profile and weighing porosity indicated by a dashed line. Large grains existing close to the plug middle might lead to the section with reduced porosity. This rock plug has a wide range of pore length from approximately 1 µm to 100 µm, indicating a highly heterogeneous pore system.

Basic parameters in NMR experiments. The duration of 90 and 180° pulses in the NMR experiments were kept to be 25 µs (to ensure the same RF-pulse frequency bandwidth) while the amplitudes were adjusted accordingly. T_1, T_2 and D-T_2 experiments were performed as routine measurements for determining the global properties of the fluid in the rock core. Relaxation time T_2 distributions were determined using the CPMG [22] pulse sequence with an echo spacing of 150 µs and 12000 echoes. A dataset with SNR=450 was acquired within a 4-scan measurement lasting 45 s. In the fast encoding T_1 measurement, the small tip angle α was set to be 5.3° and the number of small tip angle pulse is 250. The acquisition time T_{ACQ} was optimized to be 25.6 ms. The entire experiment time was 6 min within 32 scan acquisition. D-T_2 correlation distributions were obtained with a gradient duration δ = 5 ms and diffusion observation time Δ = 40 ms. The gradient G for encoding diffusion varied up to 0.4 T/m in 40 steps linearly. The echo spacing was 150 µs and the number of echoes was 12000.

Before flooding*: *static measurement. Because of the smaller impact of T_2 relaxation during the imaging encoding period, the phase-encoded T_2 method was used to extract spatially resolved T_2 profiles in the case of static fluid measurement. The spatial resolution was 1.5 mm and the number of imaging gradients m was 64. The echo spacing in the first stage T_{E1} was set to be 500 µs and the duration of phase gradient was 100 µs. The echo spacing in the second stage was set to be 150 µs and the number of echoes was 12000. With an 8-scan measurement for each imaging gradient step, phase-encoded T_2 profile datasets have been acquired within 1.5 h. For phase encoded T_1 measurement, the spatial resolution was 3 mm and the number of imaging

gradients m was 32. The data can be acquired within 3.5 h with a 32-scan measurement for each imaging gradient step.

Before flooding, the confining pressure was set to be 1000 psi by adjusting BPR 1 in the confining circuit. To study the temperature-dependence of oil properties and distribution in rock plug, the temperatures of rock sample were set to be 25°C, 55°C and 80°C with a constant flow rate of 150 mL/min for the confining fluid PFPE heated in the heating bath. During this measurement, the inlet and outlet of flooding channel were both switched off to avoid the saturated oil being driven out during providing confining pressure.

Flooding measurements. In the flooding experiment, to obtain spatially resolved D-T_2 distribution efficiently, frequency encoded imaging method was used. Parameters have been optimized to ensure comparable results obtained from frequency encoded T_2 profiles as compared to phase encoded T_2 method. The intensity of the frequency gradient g was chosen to be 12 mT/m. The number of acquired data points for each echo was 256 and the dwell time was 2 μs. This ensured the acquisition of the full echo (as determined by T_2^*, which is close to T_2 at low-field NMR measurement). The echo spacing with T_E = 800 μs was chosen accordingly to suit the acquisition of the full echo. The number of echoes was 3000. For the acquisition in the diffusion dimension, the gradient duration δ was 5 ms and the diffusion observation time Δ was 40 ms. The gradient G for diffusion encoding varied up to 0.4 T/m in 12 steps linearly. The experimental time was 20 min with a 16-scan acquisition.

To investigate the oil recovery procedure, water was injected into the oil-saturated rock core confined in the overburden cell. During the flooding experiment, to avoid water bypassing the core and travel between the core sample and confining fluid, the overburden pressure in this work was set to be at least 300 psi higher than the inlet pressure of crank pump. Therefore, the pressure before BPR 1 was kept to be 1000 psi and the initial pressure for crank pump was 700 psi. The pressure before BPR 2 was set to be 500 psi in this work. The entire flooding procedure is carried out in small individual steps as visualized on the horizontal axis in **Figure 8**. The crank pump needs to be suspended after each flooding step. Spatially resolved D-T_2 NMR measurements are carried out after there are no reading changes from these two pressure gauges between the confined rock core. The above procedure is repeated till there is no noticeable decrease of the oil signal detected as estimated from spatially resolved D-T_2 maps. Subsequently, the confining temperature of the prepared rock plug is increased and a further set of flooding and NMR measurement is performed, in order to investigate the temperature dependence of water-flooding-oil process of rock core. Three experimental temperatures, 25°C, 55°C and 80°C, will be adopted in this work.

POROSITY PROFILE AND FLUID DISTRIBUTION

Before spatially resolved measurements were performed, T_2, T_1 and D-T_2 distributions at three temperatures under 1000 psi were acquired (**Figure 5**). T_2 distributions at the three temperatures indicate two components of oil in the pore space (light component corresponds to larger T_2 value while heavy components has a smaller T_2 value). With

increasing temperature, T_2 distribution gradually shifts towards longer relaxation time, which implies decrease of oil viscosity [23, 24]. When the sample confining temperature was increased from 55°C to 80°C, the heavy component was less shifted as compared to the light counter-part, which might be caused by weaker temperature dependence as compared to light one. Compared to T_2 distributions, T_1 results obtained from rapid encoding method have only the distribution from light component. This is caused by long signal evolution time T_{ACQ} used in the signal acquisition. Likewise, T_1 values progressively increase with heating up the rock core, which suggest the decrease of oil viscosity.

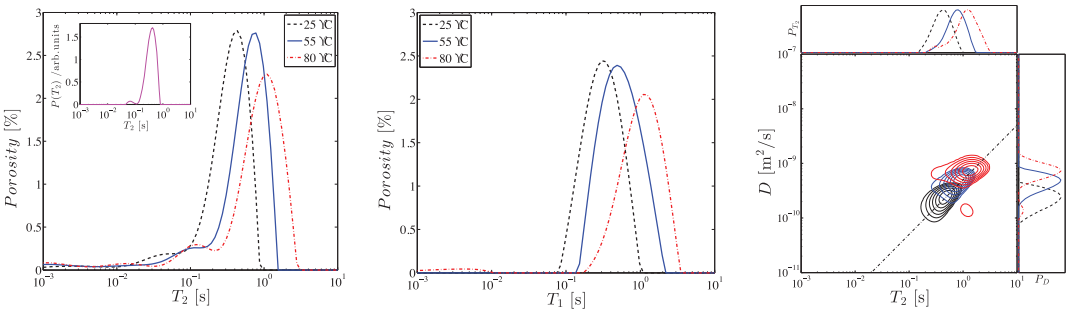

Figure 5. (**a**) Transverse relaxation T_2 and (**b**) longitudinal relaxation T_1 distributions of oil saturating rock under 1000 psi. The dash, solid and dot dash lines represent the distributions at 25°C, 55°C and 80°C respectively. The regularization factor during the inversion is 1 in T_2 and 33 in T_1 data process. (**c**) Diffusion-relaxation time correlation D-T_2 distribution under 1000 psi. The slope dash line represents hydrocarbon correlation line of D=5×10^{-10} T_2. The T_2 distribution of bulk diesel at 25°C is given in the inset of (**a**).

The diffusion-relaxation time correlation distribution were obtained and presented in Figure 5 c. Because of relaxation effect during the diffusion observation time, the heavy component with short T_2 relaxation time in the correlation experiments were missing compared to 1D relaxation results. Nevertheless, a reasonable prediction of oil properties is still accessible since the light component predominates this oil as shown in 1D T_2 spectra. Meanwhile, these 2D distributions exhibit a strong correlation between diffusion coefficient D and relaxation time T_2, a feature that is similar to that in bulk oil. It indicates non oil-wet status for this rock plug. This is probably ascribed to the thin water film absorbed at the pore walls that have not entirely dried out during the sample preparation. This amount of water, although was hardly to be detected during the experiment, results in the wettability of this rock plug. The distributions shift along the hydrocarbon line even at temperatures of up to 80°C, which proves a decrease of oil viscosity. While the shape of D and T_2 distributions remain almost the same, indicating a nearly stable composition of oil in pore space within our temperature range [24].

Spatially resolved T_1 and T_2 profiles at 25°C are presented in Figure 6 a and b, respectively. Similar features, such as the heterogeneity of porosity profile, can be observed along the cylindrical axis in both maps. Because of the long T_{ACQ} time adopted here, heavy component of oil is absent in all resolved T_1 profiles, while is still visible in T_2 profiles. Both projected T_1 and T_2 distributions are comparable with the bulk results shown in Figure 5 a and b. Furthermore, spatially resolved T_2 experiments

were performed at confining temperatures of 55°C and 80°C in order to investigate the oil temperature-dependent behaviour. The varying T_2 and spatial features as seen at 55°C and 80°C are not understood yet and remain subject to further research. However, projections onto the spatial and T_2 domains remain reasonable and confirm a shift of T_2 towards higher temperatures as expected.

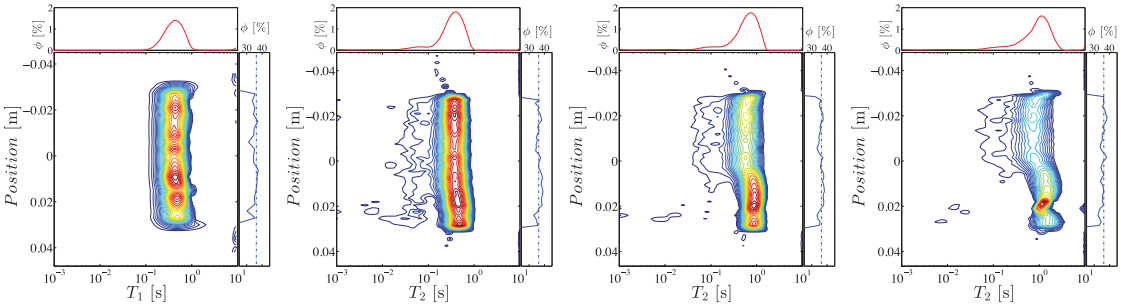

Figure 6. (**a**) Spatially resolved T_1 profile at 25°C and T_2 profiles at (**b**) 25°C, (**c**) 55°C and (**d**) 80°C under 1000 psi. The top panel presents the projected T_2 relaxation distribution and right panel gives the porosity profile. The blue dashed line in the right panel corresponds to the weighing porosity value.

In summary, the oil situated in the rock core becomes less viscous with increasing the confining temperature, which is revealed from T_1, and T_2 distributions as well as from the D-T_2 correlation distributions. The spatial T_2 profile resolves the T_2 distributions along cylindrical core dimension, also exhibiting distinct oil properties and distributions at different confining temperatures.

IN-SITU WATER-FLOODING MEASUREMENTS

In this section, multi-phase fluid transport processes at different temperatures are observed by using the spatially resolved D-T_2 technique. The oil-saturated rock plug was firstly flooded by water at 25°C and 1000 psi. Subsequently, two further flooding steps at 55°C and 80°C were performed to investigate the temperature dependence during the flooding process. The spatially resolved D-T_2 profiles before, during and after water flooding at 25°C are compared and presented in Figure 7. In order to visualize the existence of two different fluid phases, two reference planes indicating oil (left) and water (right) were added in to the figures as grey planes.

The distribution function $F(z,D,T_2)$ before water flooding (shown in Figure 7 a) mainly extends along the hydrocarbon plane indicating oil saturating from top to bottom in the rock plug. After flooding an amount of water corresponding to 0.1 pore volume through the rock (0.1 PV water flooding), there appears a distinct distribution neighbouring the oil signal and laying along water reference plane (Figure 7 b). This signal extends along the water plane after 1 PV water flooding (shown in Figure 7 c). From the reference planes, it can be distinguished that the left column represents residual oil while the right one is the injected water. Therefore, it is feasible to extract the spatially resolved residual oil and water saturation from this distribution, and estimate oil recovery efficiency. The volume of flooding water was incremented up to 2.2 PV and two subsequent flooding experiments at 55°C and 80°C were performed with equal amount of water flooding.

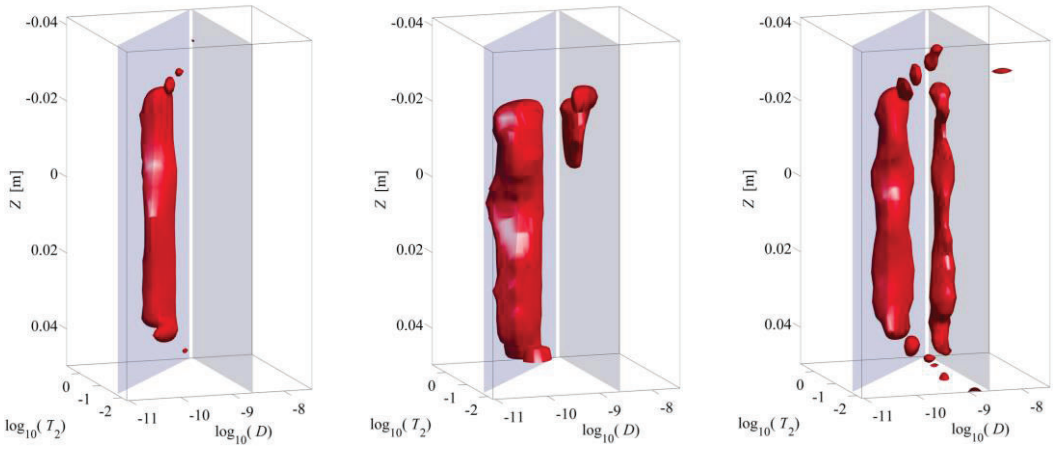

Figure 7. Spatially resolved D-T_2 profile before water flooding (**a**), and after 0.1 PV (**b**) and 1 PV (**c**) water flooding at 25°C. Two reference planes indicating hydrocarbon and water were plotted in order to identify the spatial distributions of oil and water signals.

The intensities of oil and water signals in the spatially resolved D-T_2 maps of each water flooding step can be readily summed up and plotted as relative water and oil saturation (shown in Figure 8).

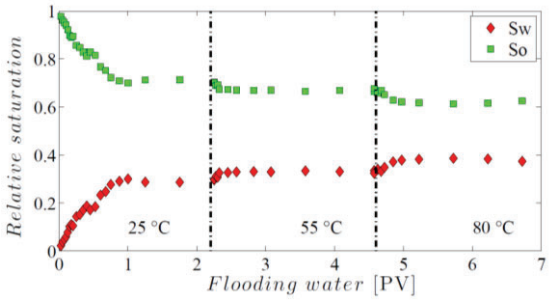

Figure 8. Relative water (red diamond) and oil (green square) saturation estimated from the spatially resolved D-T_2 maps. The entire flooding procedure is performed under three confining temperatures (25°C, 55°C and 80°C). The amount of flooding water is normalized with the pore volume (PV) of the rock plug here. During the flooding in each temperature, the water volume is incremented to 2.2 PV.

For the water-flooding procedure at 25°C, the relative oil saturation drops rapidly with increasing the flooding water volume, and reaches to a plateau level after 1 PV water injection. The further flooding shows no obvious oil yield in this rock plug. By increasing the rock temperature, the relative oil saturation continues to decrease because of the higher oil mobility, and quickly converges to a constant level afterwards. The residual oil saturation is still above 50% even at rock temperatures up to 80°C, which is a higher value as compared to common water-flooding-oil experiments (lower than 40% of residual oil saturation). This may due to the relatively high flow rate of the flooding water (approximately 0.25 mL/s) provided by the crank pump in this case. In order to investigate the multi-phase fluid interaction, all distributions under three temperatures were projected into the D-T_2 dimension and shown in Figure 9.

Regardless of longitudinal relaxation during the diffusion observation time, the ratio of water and oil varies gradually with increasing the rock temperature, which can be observed from the projected diffusion coefficients in the right panel of each distribution. These results exhibit the same features as shown in the relative saturation data in Figure 8, and imply a process of enhanced oil recovery by flooding the rock

plug at higher temperatures. Further oil recovery strategy, such as gas, thermal or chemical polymer injection may be justified.

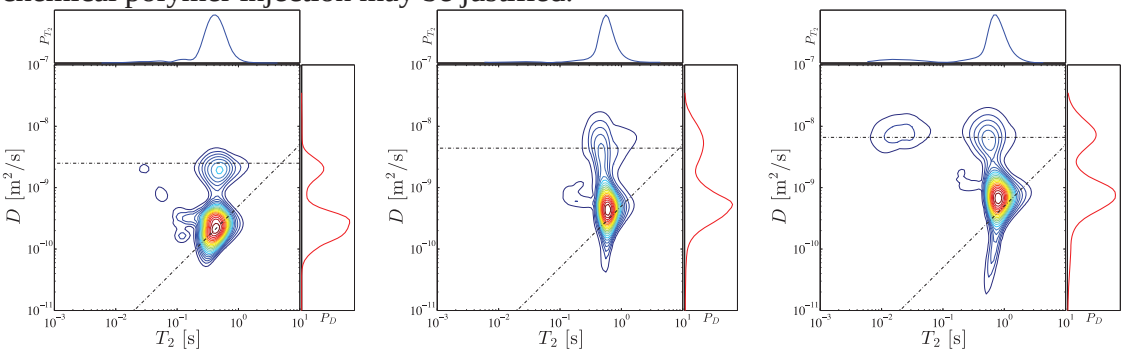

Figure 9. Projected diffusion-relaxation correlation distribution at (**a**) 25°C, (**b**) 55°C and (**c**) 80°C. The horizontal lines represent water diffusion coefficient at 25°C (=2.3×10^{-9} m^2/s), at 55°C (=4.4×10^{-9} m^2/s), and at 80°C (=6.6×10^{-9} m^2/s) [25]. The slope dash line represents hydrocarbon correlation line of D=5×10^{-10} T_2. The top panel presents the projected relaxation distribution and right panel shows the projected diffusion coefficient distribution.

CONCLUSION

Based on the constructed high pressure/temperature NMR measuring system, spatially resolved T_1 and T_2 relaxation techniques provides direct insight into local properties of fluid situated in the pores of rock core at reservoir-like conditions. Furthermore, a spatially resolved D-T_2 method yields substantial information regarding flooding experiments, such as wetting status, residual oil/water saturation profiles, and their dependence on temperature. The current hardware set-up and the implemented NMR methods provide the base for further investigations of the residual oil saturation and displacements in the context of enhancement oil recovery.

ACKNOWLEDGEMENTS

The project was supported by the New Zealand Ministry of Business, Innovation, and Employment via the Grant "New NMR Technologies". Magritek Ltd. is acknowledged for providing the overburden cell. R. Peterson (Daedalus Innovations LLC), S. Buchanan (Magritek Ltd.) and T. Brox (VUW) are acknowledged for the technical suggestions. H-B. Liu thanks the financial supports from Chinese Scholarship Council (CSC).

REFERENCES

1. Dunn, K.-J., D.J. Bergman, G.A. Latorraca, *Nuclear magnetic resonance: Petrophysical and logging applications*, Pergamon, (2002).
2. Mitchell J., L.F. Gladden, T.C. Chandraseker, E.J. Fordham, "Low-field permanent magnets for industrial process and quality control," *Progress in Nuclear Magnetic Resonance Spectroscopy*, (2014) 76, 1–60
3. Hürlimann M.D, "The diffusion–spin relaxation time distribution function as an experimental probe to characterize fluid mixtures in porous media," *The Journal of chemical physics*, (2002) 117, 22, 10223–10232.
4. Sun, B.Q., M. Olson, J. Baranowski, S. Chen, W. Li, D. Georgi, "Direct fluid typing and quantification of Orinoco Belt heavy oil reservoirs using 2D NMR logs", *SPWLA 47th Annual Logging Symposium*, Veracruz, Mexico, June 4-7, (2006).

5. Hürlimann, M.D., M. Flaum, L. Venkataramanan, C. Flaum, R. Freedman, G.J. Hirasaki, “Diffusion-relaxation distribution functions of sedimentary rocks in different saturation states,” *Magnetic Resonance Imaging*, (2003) 21,3-4, 305–310.
6. Kim, K., S.-H. Chen, F.-F. Qin, A.T. Watson, "Use of NMR Imaging for determining fluid saturation distributions during multiphase displacement in porous media." *International Symposium of the Society of Core Analysis*, (1992) 9219.
7. Sun B.-Q., K.-J. Dunn, G.A. LaTorraca, D.M. Wilson, “NMR imaging with diffusion and relaxation,” *International Symposium of the Society of Core Analysts*, Pau, France, September 21-24, (2003), SCA2003-24.
8. Rauschhuber, M., G. Hirasaki, “Determination of saturation profiles via low-field NMR imaging,” *International Symposium of the Society of Core Analysts*, Noordwijk, Netherlands, September 27–30, (2009), SCA2009-09.
9. Mitchell, J., “Magnetic resonance core analysis at 0.3 T,” *International Symposium of the Society of Core Analysts*, Avignon, France, September 8–11, (2014), SCA2014-10.
10. Utracki, L.A., “Temperature and pressure dependence of liquid viscosity,” *The Canadian Journal of Chemical Engineering*, (1983) 61, 5, 753-758.
11. Dandekar A.Y., *Petroleum reservoir rock and fluid properties*, CRC press, (2013).
12. Tiab D., E.C. Donaldson, *Petrophysics: theory and practice of measuring reservoir rock and fluid transport properties*, Gulf professional publishing, (2011).
13. http://www.magritek.com.
14. http://www.daedalusinnovations.com/apparatus/rockcore.html.
15. Callaghan, P.T., *Principles of nuclear magnetic resonance microscopy*, Oxford University Press, Inc., New York, (1991).
16. Perlo J., F. Casanova, and B. Blümich, “3D imaging with a single-sided sensor: an open tomograph”, *Journal of Magnetic Resonance*, (2004) 166, 228–235.
17. Hsu, J.-J., I. J. Lowe, “Spin-lattice relaxation and a fast T_1-map acquisition method in MRI with transient-state magnetization”, *Journal of Magnetic Resonance*, (2004) 169, 270-278.
18. Chandrasekera T.C., J. Mitchell, "Rapid encoding of T_1 with spectral resolution in n-dimensional relaxation correlations", *Journal of Magnetic Resonance*, (2008) 194, 1, 156-161.
19. Tanner, J.E., "Use of the stimulated echo in NMR diffusion studies," *The Journal of Chemical Physics*, (1970) 52, 5, 2523-2526.
20. Venkataramanan, L., M.D. Hürlimann, Y-Q. Song, “Solving Fredholm integrals of the first kind with tensor product structure in 2 and 2.5 dimensions,” *IEEE Transactions on Signal Processing*, (2002) 50, 5, 1017–1026.
21. Song, Y.-Q., S. Ryu, P. N. Sen, “Determining multiple length scales in rocks”, *Nature*, (2000) 407, 178-181.
22. Meiboom, S., D. Gill, "Modified spin-echo method for measuring nuclear relaxation times," *Review of Scientific Instruments*, (1958) 29, 8, 688-691.
23. Freed, D.E., M.D. Hürlimann, “One-and two-dimensional spin correlation of complex fluids and the relation to fluid composition,” *Comptes Rendus Physique*, (2010) 11, 2, 181–191.
24. Freed, D.E., “Temperature and pressure dependence of the diffusion coefficients and NMR relaxation times of mixtures of alkanes”, *The Journal of Physical Chemistry B*, (2009) 113, 13, 4293-4302.
25. Holz, M., S. R. Heil, A. Sacco, “Temperature-dependent self-diffusion coefficients of water and six selected molecular liquids for calibration in accurate ^{1}H NMR PFG measurements”, *Physical Chemistry Chemical Physics*, (2000) 2, 4749-4742.